Title
STOIC: a study of coupled model climatology and variability in tropical ocean regions

Journal
Climate Dynamics, 18(5)

ISSN
0930-7575

Authors
Davey, M
Huddleston, M
Sperber, K
et al.

Publication Date
2002

DOI
10.1007/s00382-001-0188-6

Climate Dynamics (2002) 18: 403–420
DOI 10.1007/s00382-001-0188-6

**M.K. Davey · M. Huddleston · K.R. Sperber
P. Braconnot · F. Bryan · D. Chen · R.A. Colman
C. Cooper · U. Cubasch · P. Delecluse · D. DeWitt
L. Fairhead · G. Flato · C. Gordon · T. Hogan · M. Ji
M. Kimoto · A. Kitoh · T.R. Knutson · M. Latif
H. Le Treut · T. Li · S. Manabe · C.R. Mechoso
G.A. Meehl · S.B. Power · E. Roeckner · L. Terray
A. Vintzileos · R. Voss · B. Wang · W.M. Washington
I. Yoshikawa · J.-Y. Yu · S. Yukimoto · S.E. Zebiak**

STOIC: a study of coupled model climatology and variability in tropical ocean regions

Received: 12 September 2000 / Accepted: 20 June 2001 / Published online: 7 December 2001

Abstract We describe the behaviour of 23 dynamical ocean-atmosphere models, in the context of comparison with observations in a common framework. Fields of tropical sea surface temperature (SST), surface wind stress and upper ocean vertically averaged temperature (VAT) are assessed with regard to annual mean, seasonal cycle, and interannual variability characteristics. Of the participating models, 21 are coupled GCMs, of which 13 use no form of flux adjustment in the tropics. The models vary widely in design, components and purpose: nevertheless several common features are apparent. In most models without flux adjustment, the annual mean equatorial SST in the central Pacific is too cool and the Atlantic zonal SST gradient has the wrong sign. Annual mean wind stress is often too weak in the central Pacific and in the Atlantic, but too strong in the west Pacific. Few models have an upper ocean VAT seasonal cycle like that observed in the equatorial Pacific. Interannual variability is commonly too weak in the models: in particular, wind stress variability is low in the equatorial Pacific. Most models have difficulty in reproducing the observed Pacific 'horseshoe' pattern of negative SST correlations with interannual Niño3 SST anomalies, or the observed Indian-Pacific lag correlations. The results for the fields examined

M.K. Davey (✉) · M. Huddleston · C. Cooper · C. Gordon
Meteorological Office, Bracknell, London Road,
Bracknell RG12 2SZ, UK
E-mail: mike.davey@metoffice.com

K.R. Sperber
PCMDI, Lawrence Livermore National Laboratory,
Livermore, CA, USA

P. Braconnot
Laboratoire de Modelisation du Climat et de
l'Environnement, France

F. Bryan · W.M. Washington · G.A. Meehl
National Center for Atmospheric Research, Boulder, CO, USA

D. Chen · D. DeWitt · S.E. Zebiak
Lamont Doherty Earth Observatory, Palisades, NY, USA

R.A. Colman · S.B. Power
Bureau of Meteorology Research Centre, Melbourne, Australia

U. Cubasch · R. Voss
Deutsches Klimarechenzentrum, Hamburg, Germany

P. Delecluse
LODYC-ISPL, Paris, France

L. Fairhead · H. Le Treut · A. Vintzileos
Laboratoire de Meteorologie Dynamique, Paris, France

G. Flato
Canadian Centre for Climate Modelling and Analysis,
Victoria, Canada

T. Hogan · T. Li
Naval Research Laboratory, Monterey, CA, USA

M. Ji
National Centers for Environmental Prediction,
Camp Springs, MD, USA

M. Kimoto
Center for Climate System Research, Tokyo, Japan

A. Kitoh · S. Yukimoto
Meteorological Research Institute, Tsukuba, Japan

T.R. Knutson
Geophysical Fluid Dynamics Laboratory,
Princeton, NJ, USA

M. Latif · E. Roeckner
Max-Planck-Institut für Meteorologie,
Hamburg, Germany

S. Manabe
Earth Frontier Research System, Tokyo, Japan

C. R. Mechoso · J.-Y. Yu
University of California Los Angeles, USA

L. Terray
CERFACS, Toulouse, France

B. Wang
University of Hawaii, Honolulu, HI, USA

I. Yoshikawa
Japan Meteorological Agency, Tokyo, Japan

indicate that several substantial model improvements are needed, particularly with regard to surface wind stress.

1 Introduction

The tropics are regions of strong ocean-atmosphere interaction on seasonal and interannual time scales, so a good representation of observed tropical behaviour is a prime objective for coupled ocean-atmosphere models. As previous assessments focusing on the tropical Pacific have established (Mechoso et al. 1995 for SST and precipitation seasonal cycles; Neelin et al. 1992 for SST interannual variability; see also the review by Delecluse et al. 1997), it is difficult to develop coupled general circulation models (CGCMs) with the right balance of oceanic and atmospheric processes and interactions in the tropics. These assessments found that systematic errors in sea surface temperature (SST) were often largest in the equatorial Pacific, and model representations of El Niño Southern Oscillation (ENSO) variability were often weak and/or incorrectly located.

To broaden and update the previous assessments, two companion projects were initiated by the CLIVAR Numerical Experimentation Group 1 (NEG1): the El Niño Simulation Intercomparison Project (ENSIP) and the Study of Tropical Oceans In CGCMs (STOIC). (NEG1 has subsequently evolved into the CLIVAR Working Group on Seasonal to Interannual Prediction, WGSIP.) SST, surface wind stress and upper ocean vertically averaged temperature (VAT) data from 21 CGCMs and two intermediate coupled models (Table 1) were gathered, along with observational analyses. These variables were selected because they are key ingredients in tropical ocean-atmosphere dynamics, in that SST strongly influences tropical atmospheric circulation; surface wind stress drives the upper ocean circulation; the upper ocean supports large-scale internal waves that can transfer information long distances and influence SST.

The aim was to compare the various models against observations, to identify common weaknesses and strengths. Results from ENSIP, concentrating on the equatorial Pacific, have been described by Latif et al. (2001) (hereafter ENSIP2001), while the results from STOIC are the subject of this work. The STOIC analyses extend beyond the equatorial Pacific, to examine behaviour in all three tropical ocean regions (Atlantic, Indian and Pacific), including inter-ocean relationships. Further results and an extensive set of figures are provided in a separate detailed report (hereafter STOIC2000, see Davey et al. 2000 or contact the lead author). Many of the models have also been assessed collectively as part of the Coupled Model Intercomparison Project (CMIP, Meehl et al. 2000): in particular, ENSO behaviour from an atmospheric viewpoint is described in AchutaRao et al. (2001). The ENSIP and STOIC projects, focusing on tropical ocean regions, are separate from CMIP.

From the submitted data, annual means, annual cycles and interannual anomalies were calculated. Here 'interannual anomaly' means the value of a variable with the monthly climatology subtracted. To be specific: suppose the SST for year i and month m in a 20-year

Table 1 Model details

Label	Model	Atmos grid Lat × Long	Ocean grid Lat × Long	Coupled domain
A	BMRC	R21 L19	0.5-5.9 ×2.0 L25	Global
. a	CCC	T32 L10	1.8 ×1.8 L29	Global
B	CCSR	T21 L20	0.5-2.0 ×2.5 L20	Global
C	CERFACS	T42 L31	0.33-1.5 ×0.75 L28	Tropical Pacific
D	COLA	T30 L18	1.0-3.0 ×3.0 L20	Tropical Pacific - Atlantic
. b	DKRZ-OPYC	T42 L19	0.5-2.8 ×2.8 L11	Global
. c	DKRZ-LSG	T21 L19	4.0 ×4.0 L11	Global
. d	GFDL-R15	R15 L9	3.75 ×4.5 L12	Global
. e	GFDL-R30	R30 L14	2.2 ×1.875 L18	Global
. f	HAWAII	1.0 ×2.0 L2	1.0 ×2.0 L2	Tropical Pacific
E	IPSL-TOGA	50points ×5.6 L11	0.33-1.5 ×0.75 L28	Tropical Pacific
F	IPSL-HR	72points ×3.75 L15	0.5-1.5 ×2.0 L31	Global
G	IPSL-LR	50points ×5.6 L11	1.0-3.0 ×4.0 L31	Global
H	JMA	T42 L21	0.5-2.0 ×2.5 L20	Global
. g	LAMONT	2.0 ×5.625 1 vertical mode	0.5 ×2.0 L2	Tropical Pacific
I	METO-CM3	2.5 ×3.75 L19	1.25 ×1.25 L20	Global
J	MPI	T42 L19	0.5-2.8 ×2.8 L20	Global
. h	MRI	4.0 ×5.0 L15	0.5-2.0 ×2.5 L21	Global
K	NCAR-CSM	T42 L18	1.2 ×2.4 L45	Global
L	NCAR-WM	R15 L9	1.0 ×1.0 L20	Global
. i	NCEP	T42 L18	0.33-1.0 ×1.5 L28	Tropical Pacific
. j	NRL	T39 L12	0.5-2.0 ×2.0 L25	Tropical Pacific
M N	UCLA-PAC UCLA-ATL	3.0 ×5.0 L15	0.33 ×1.0 L27	Tropical Pacific, Tropical Atlantic

Ln denotes n vertical levels. Atmosphere: Rn and Tn denote rhomboid and triangular spectral horizontal resolution. Ocean: A-B denotes irregular oceanic latitudinal resolution with grid spacing A at the equator increasing poleward to B. The IPSL models use AGCMs with a Gaussian meridional grid distribution. The labels are upper case for 'no-adjustment' and lower case for 'flux-adjusted' models

sample is denoted SST_{im}. Then the annual mean is the average of all years and months: $\Sigma_i \Sigma_m SST_{im}/12*20$. The monthly climatology for month m is $SST_m = (\Sigma_i SST_{im}/20)$, and the interannual anomaly for month m of year i is $SST'_{im} = SST_{im} - SST_m$.

It is impractical to present full details of the behaviour of each model. The intention instead is to highlight and summarise some particular features. To this end, zonal and meridional sections and area-averages (Table 2) have been selected to allow ready comparison of the models with the observations, as described in the following sections.

2 The models and observational data

The basic data provided for STOIC were monthly mean fields of tropical SST, surface wind stress, and upper ocean heat content from typical 20 year periods of coupled integration. Most data were submitted in 1997, with some in 1998. In the cases where more than 20 years of data were submitted, the analyses have been based on the last 20 years only. The spatial coverage of the data provided also differed between models, ranging from equatorial strips in individual oceans to globally complete fields. Note that the model integrations were not conducted under standardised conditions, so for example initial states, lengths of integration and coupling strategies differ from case to case.

The models vary considerably in configuration. Some basic information is provided in Table 1 and Appendix A, and further details may be found in ENSIP2001. Many of the models have been analysed individually and are described in separate publications (see Appendix A). Some have relatively low resolution, and are designed for multi-century integrations for low frequency climate variability research, while others have high resolution (particularly in the oceanic equatorial regions) and are aimed at seasonal scales.

For convenience of presentation and comparison, a division into models with and without some form of flux adjustment has been made, as indicated in Table 1: these two groups will be referred to as 'adj' and 'no-adj' respectively. The CCSR model is placed in the 'no-adj' group as it has SST relaxation only in polar regions. The majority have no form of surface 'flux adjustment' (here we use the term liberally to include e.g. relaxation to observed SST, or anomaly coupling, as well as fixed flux alterations). Among the flux-adjusted group, the nature and degree of adjustment varies in each model: some are more tightly constrained to observed climatology than others, and they are not all constrained by the same climatologies.

For a few CGCMs separate datasets were submitted for different oceanic regions, as indicated by the labels in some figures. While for the COLA, NCAR-WM and NCAR-CSM models the data are from a single CGCM respectively, for UCLA there are separate Pacific (UCLA-PAC) and Atlantic (UCLA-ATL) models with different atmospheric as well as oceanic components.

For comparison, monthly gridded datasets based on analyses of observations were obtained from various sources: SST for 1871-1999 from the Met Office GISST3 SST/sea-ice dataset on a 1°×1°grid (Rayner et al. 1998); surface wind stress for 1980-1993 from the Southampton Oceanography Centre dataset (Josey et al. 1999) and for 1950-1989 from the WM-COADS dataset (Da Silva et al. 1995) on 1°×1°grids; and upper ocean heat content from Scripps Institution of Oceanography (Tourre and White 1997) on a 2°latitude ×5°longitude grid for 1950-1998.

The GISST3 dataset is sufficiently long for an assessment of the observed behaviour in different 20-year segments to be made, bearing in mind however that the density of observations varies considerably with time. To illustrate how analysed values from 20-year samples can vary, 20-year running mean values of standard deviation for SST in the Pacific Niño3 region range from 0.55 (1940-60) to 0.95 (1970-90). This range of natural variability has to be borne in mind when assessing the models.

3 Annual mean climatology

Comparisons between observations and models along equatorial and meridional sections are provided in this section. The equatorial Pacific region is discussed in more detail in ENSIP2001.

3.1 SST

Annual mean SST calculated in an equatorial 2N-2S strip is shown in Fig. 1, separated into the 'no-adj' and 'adj' groups, along with the observed annual mean from the 1961-90 GISST3 climatology. In the Pacific sector, an important feature is that the strong east-west SST gradient is by and large correct in all model: in early generations of 'no-adj' CGCMs, that gradient was often much flatter or even reversed. However, most 'no-adj' models have a systematic cold bias (2 °C or more in many cases) over much of the equatorial Pacific. East of 260°E, the observed mean SST rises approaching the South American coast. Most 'no-adj' models exaggerate this rise, with substantial positive SST errors common in this region. From other assessments, the warm SST errors adjacent to the South American coast in CGCMs are typically linked to errors in the simulation of stratus cloud, with loss of cloud cover associated with increased solar radiation into the ocean.

In the Atlantic sector, observed mean SST decreases eastward from the American coast, rising again east of 10°W approaching the African coast. In nearly all the 'no-adj' models the SST is biased cold in the west equatorial Atlantic, by up to 3 °C, but biased warm in

Table 2 Definitions of regions used for area averages. Those in the right column are for the composite wind stresses

Label			Label		
Niño3	5N–5S	150W–90W	EqPac1	10N–10S	160E–120W
PacCen	5N–5S	165E–225E	EqPac2	10N–equ	160E–120W
PacW	2N–2S	130E–160E	EqPac3	0–10S	160E–120W
PacN	15N–30N	150E–180E	EPac	0–10N	120W–80W
PacS	15S–30S	160E–190E	NPac	25N–35N	160E–130W
IndCen	0–10N	60E–80E	SPac	25S–35S	160E–160W
			EqInd	5N–5S	70E–110E
AtlCen	5N–5S	15W–35W	SInd	20S–30S	70E–110E
AtlN	10N–20N	20W–60W	EqAtl	5S–5N	50W–30W

the east equatorial Atlantic. As in the Pacific, the SST rise approaching the African coast is exaggerated, with reduced stratus cloud a likely symptom. Of the 'no-adj' CGCMs, all except COLA have the SST gradient in the central equatorial Atlantic (40°W to 10°W) opposite to that observed.

In the equatorial Indian ocean the 'no-adj' CGCMs generally have the right zonal gradient, with SST rising rapidly eastward from relatively cold levels at the African coast, where upwelling of cold water occurs during the boreal summer season. As in the Pacific, most 'no-adj' models have a cold bias. METO-CM3 is an exception, with a warm Indian sector bias that connects to a very warm far west Pacific SST bias.

Within the 'adj' group, DKRZ-LSG stands out as consistently about 3 °C too cool in each ocean: note

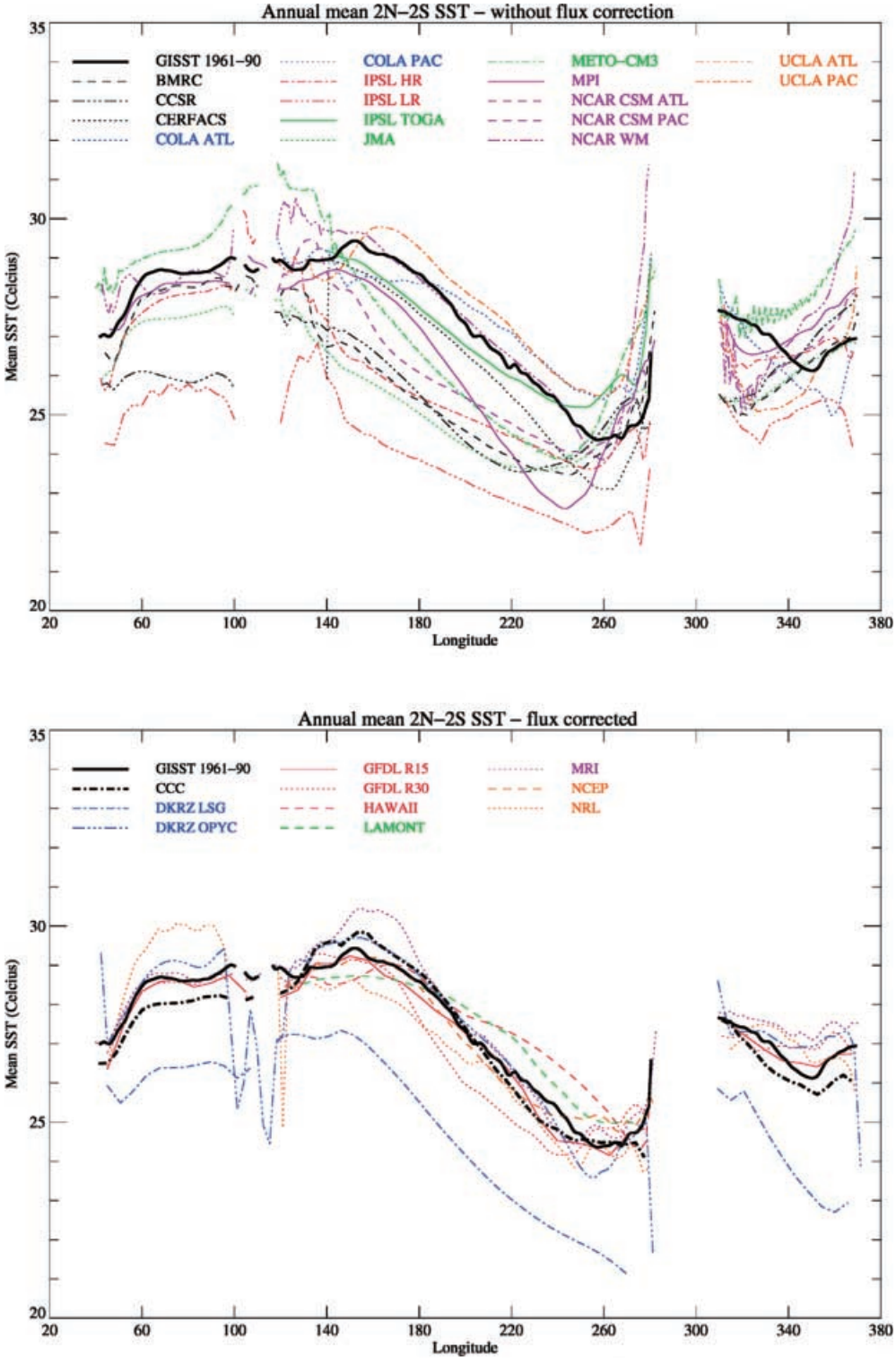

Fig. 1 Annual mean SST zonal section for the equatorial strip 2°N-2°S, as observed and for (*top panel*) 'no-adj' and (*bottom*) 'adj' models

however that DKRZ-LSG is not intended for tropical climate simulation. Among the other 'adj' models, positive and negative errors of up to 1 °C can be found in each ocean: the biases here depend on the degree and nature of the adjustments imposed. The errors are not necessarily consistent between basins: NRL has a positive bias in the Indian ocean, but a negative bias in most of the Pacific. MRI is close to observed SST in the Indian Ocean, but is substantially too warm around the dateline in the Pacific.

The east Pacific 'cold tongue' is a major observed SST feature, and a meridional section from 30°N to 30°S, averaged over 100°W-110°W, was calculated to check the performance of the models in this respect (see STOIC2000). The observations have a mean 'cold tongue' minimum slightly south of the equator, embedded within a general trend of SST increasing from 30°S to a maximum near 15°N. While most 'no-adj' models are too cool on the equator, most are too warm just off the equator near 5°S (particularly) and 5°N: consequently most 'no-adj' models have a much more pronounced cold tongue than that observed. All have maximum SST north of the equator, as observed. Nearly all have clear north-south asymmetry - the main exceptions being BMRC, which is nearly symmetric, and NCAR-WM which has a large warm bias on both sides of the equator.

An Atlantic meridional section averaged over 20°W-30°W was likewise calculated. In contrast to the east Pacific section, here there is only a very weak observed minimum in annual mean SST at the equator, and SST is broadly symmetric about the equator. Among the 'no-adj' CGCMs, MPI simulates the observed climatology very well, while most others have a minimum at the equator that is deeper than observed. Two of this group (NCAR-WM, METO-CM3) are strongly asymmetric, with an SST maximum north of the equator up to 2°C larger than observed.

For the Indian Ocean a meridional section averaged over 60°E-70°E was calculated. The observations have no equatorial minimum, and SST steadily decreases northward and southward from a flat maximum near 1°N. Most of the 'no-adj' CGCMs have an SST pattern broadly similar to that observed. Two (CCSR, NCAR-WM) clearly have an erroneous near-equatorial cold tongue feature.

3.2 Zonal wind stress

Annual mean zonal wind stress was calculated for a 5°N-5°S equatorial belt. The SOC climatology is an average for 1980-93, whereas the WM-COADS climatology is for 1970-89. The two climatologies are in close agreement, with the main difference in the west Pacific, as can be seen in Fig. 2. The mean equatorial winds are easterly over the Pacific and Atlantic oceans (except near the eastern boundaries), and westerly over the Indian Ocean (except near the African coast).

Results for the 'no-adj' CGCMs (Fig. 2a) are most varied in the central and west Pacific, where all models (with the exception of CERFACS) differ substantially from the observations. In the central Pacific (180°E to 240°E) the easterly wind stresses are underestimated by many models, whereas in the west Pacific (west of 160°E) the wind stress is strongly easterly in most models, instead of near zero as observed. The substantial wind stress gradient (increasing easterlies from 130°E to 200°E) is missed by all but CERFACS. The model biases are much larger than the difference between the SOC and WM-COADS observations. By contrast, the model wind stresses are close to the observations in the east equatorial Pacific (east of 100°W).

These 'no-adj' model wind stress errors are co-located with systematic SST errors seen in Fig. 1, which are also large in the west-central Pacific. Note however that the two models with the best central Pacific SST (COLA and NCAR-WM) have the weakest central Pacific wind stresses! In general, the 'no-adj' CGCMs have both too-cool SST and too-weak easterly wind stress in the central equatorial Pacific. The 'obvious' cold bias explanation (equatorial SST too cold because local easterlies and upwelling are too strong) does not seem to apply. Similar behaviour was noted in the earlier assessment by Mechoso et al. (1995).

In the equatorial Atlantic nearly all the 'no-adj' models have wind stresses that are much weaker than observed: only COLA has the right strength. However, the zonal gradients are quite similar to that observed, which is surprising in view of the poor zonal SST gradients described above (Fig. 1). Further investigation is needed to explain this contrast in wind stress and SST gradient performance. Part of the explanation may be that in the Atlantic the equatorial wind stresses are controlled more by off-equatorial factors such as SST distribution, and the location and strength of convection centres. The weakened easterlies may be connected with shifts in the main convection centres in the east Atlantic that are associated with warm SST biases in that region. Over the Indian Ocean several of the 'no-adj' models have weaker westerly zonal wind stress than observed. Three (CCSR, IPSL-LR, IPSL-HR) have mean easterlies throughout the equatorial Indian Ocean sector. As described in more detail after, the errors are more evident in the boreal summer monsoon season.

Wind stress results for the 'adj' models are provided in Fig. 2b. The gradients of the model wind stresses are quite similar to those observed in the Pacific and Atlantic sectors, but there are substantial differences in strength. The magnitudes of the model Pacific easterly maxima (correctly located near 210°E) vary substantially, from 0.04 to 0.08 N m^{-2} compared with the observed value of 0.055 N m^{-2}. These discrepancies reflect differences in the atmospheric components of the models: the highest (DKRZ-OPYC) and lowest (CCC) magnitudes are both for models with SST kept close to

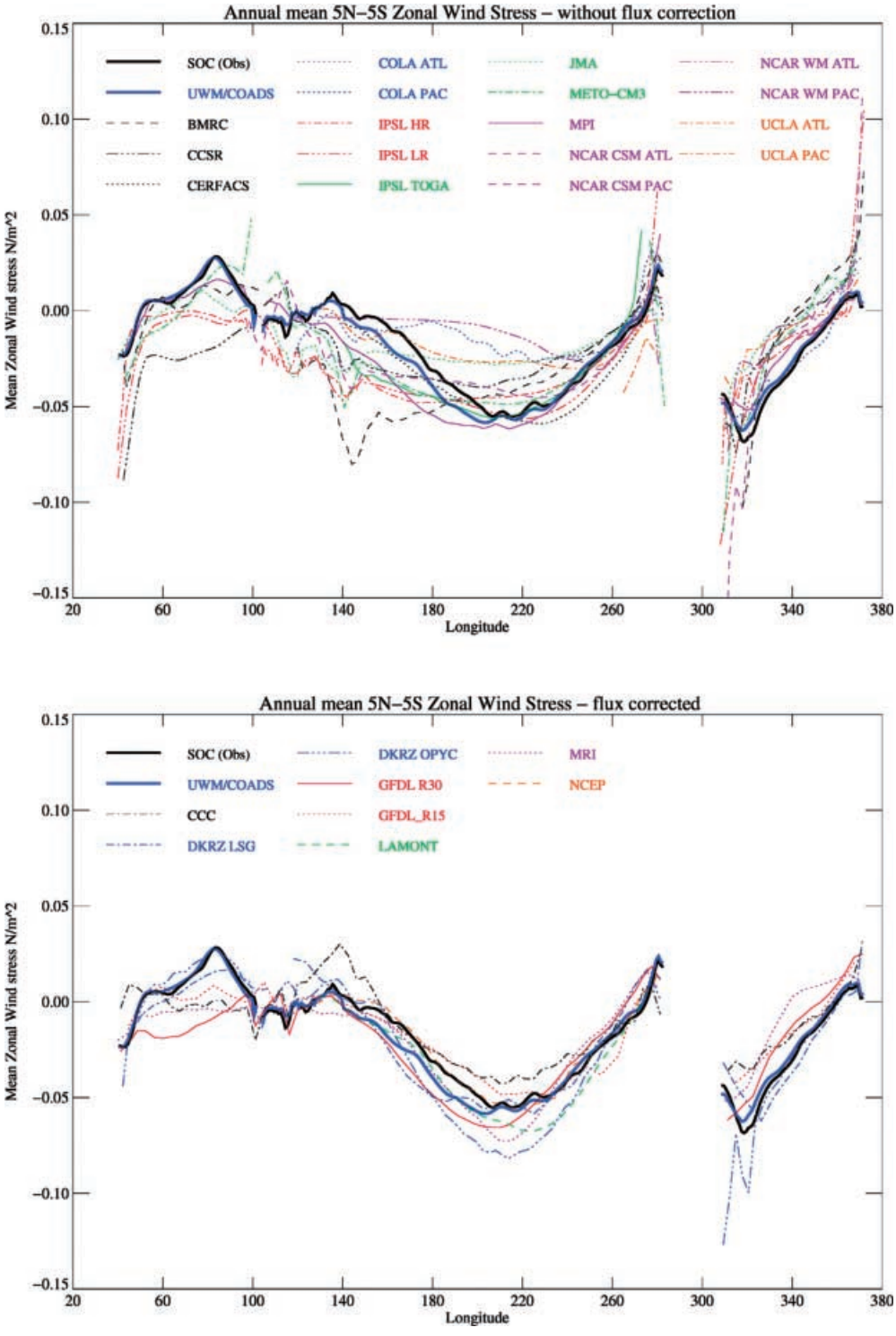

Fig. 2 Annual mean zonal wind stress zonal section in the equatorial strip 5°N-5°S, as observed and for (*top*) 'no-adj' CGCMs, (*bottom*) 'adj' CGCMs

the observed climatology (Fig. 1). In the central equatorial Atlantic the DKRZ-OPYC and DKRZ-LSG model wind stresses match the observations closely, but the other 'adj' CGCMs substantially underestimate the magnitude of the easterlies. In the Indian sector, most 'adj' CGCMs substantially underestimate the westerly wind stress in the central Indian Ocean, and a few (GFDL-R30, MRI, CCC) have mean easterlies in this area.

4 Seasonal cycles

4.1 Equatorial SST

Time-longitude plots of the seasonal cycle of Pacific SST along the equator (with the annual mean removed) are provided and discussed in detail in ENSIP2001: the largest seasonal equatorial Pacific SST errors tend to

occur in the east Pacific toward the American coast. Here we describe equivalent time-longitude diagrams (not shown here) for the equatorial SST seasonal cycle for the Atlantic and Indian oceans.

In the Atlantic sector the annual cycle is dominant in the observations: it is strongest in the east, with a maximum range of 5°C around longitude 10°W, and quite weak in the west Atlantic. There is no clear zonal propagation. Values are positive from November-April, and negative May-September, with a rapid transition in April. Most of the 'no-adj' CGCMs also have dominant Atlantic annual cycles, the main exceptions being JMA and IPSL-LR which have dominant semi-annual cycles. With regard to the longitude of the maximum seasonal range, the majority correctly place this in the east Atlantic: the exceptions are NCAR-WM and METO-CM3 (both with a central Atlantic maximum extending to the American coast); IPSL-LR (maximum range in the west Atlantic); DKRZ-OPYC (very strong reversed cycle at the American coast), and DKRZ-LSG (strong cycle next to the African coast). The seasonal range of most of the 'no-adj' models is weaker than observed; about 50% or less for CCSR, IPSL-LR, METO-CM3 and NCAR-CSM. Overall, of the 'no-adj' group the COLA CGCM best matches the observed Atlantic seasonal cycle. The 'adj' models are constrained to be near the observed cycle.

In the equatorial Indian Ocean the observed maximum seasonal range is near 50°E, and there is a clear (but not dominant) semiannual component in the western sector between the African coast and 60°E. The main warm season is February-April and the main cool season is June-August. In the central and east Indian Ocean regions a weak annual cycle is dominant, with a warm February-April season matching the main western warm period. The only clear zonal propagation signal is eastward, east of 80°E. Of the 15 CGCMs providing Indian Ocean data, 14/15 have the largest seasonal range near the African coast as observed: the exception is CCSR, which has largest range in the eastern sector. The majority of the models in the 'adj' and 'no-adj' groups are able to represent the main pattern of seasonal features well. A few models (CCSR, DKRZ-LSG, IPSL-HR, NRL) do not have a clear western semiannual component. JMA has a dominant semiannual cycle right across the Indian Ocean, and IPSL-LR and IPSL-HR have the wrong phase in the western sector. With regard to amplitude, 8/15 have a western sector maximum substantially lower (below 1.5 °C) than that observed (over 2 °C), while 2/15 (CCSR and MPI) have a western sector minimum above −1 °C (observed below −1.5 °C).

4.2 Zonal wind stress

Time-longitude maps of the seasonal cycle of zonal wind stress in the equatorial Pacific, averaged 5N-5S, with the annual mean (Fig. 2) removed, are provided in Fig. 3. The SOC (1980-93) and COADS (1950-89) observations both reveal westward propagation with a dominant annual cycle. The maximum is in February-March in the east Pacific, moving to the west Pacific by September-October. (Note over most longitudes the annual mean zonal wind stress is easterly, so the annual cycle maximum corresponds to weaker easterly stresses.) A semi-annual component is also evident in SOC and (more weakly) in COADS in the region around 180-130°W.

The majority of the 17 CGCMs providing Pacific wind stress data have an east-to-west phase propagation pattern qualitatively like that observed, though the mix of annual and semi-annual cycles makes this obscure in some cases. NCAR-WM has a very weak seasonal cycle everywhere except close to the east coast, but most of the other CGCMs have a stronger cycle than that observed. Several (e.g. COLA, DKRZ-OPYC, IPSL-LR, JMA, MPI, NCAR-CSM) have a semiannual component that is substantially stronger and more extensive than in the SOC and COADS data. One particular feature in Fig. 3 is that for several models the annual variations near the dateline in June-July-August have moderate easterly values when the observed seasonal mean is weak westerly.

In the central equatorial Atlantic zonal wind stress seasonal cycles (not shown) were compared in the AtlCen region (5°N-5°S, 15°W-35°W). In this region the observations are easterly all year, ranging from $-0.025\ \mathrm{N\,m^{-2}}$ in February-March-April to $-0.045\ \mathrm{N\,m^{-2}}$ in the second half of the year. Most of the CGCMs have large errors in this region. In the 'no-adj' group 10/11 CGCMs have wind stresses close to zero (within $0.005\ \mathrm{N\,m^{-2}}$) or westerly for part of the first half of the year: only COLA has good year-round strength. Among the six 'adj' CGCMs that provided Atlantic wind stress data, only DKRZ-OPYC and DKRZ-LSG resemble the observations in phase and strength. The others have low strength, and one (MRI) has westerly winds in April-May.

For the Indian Ocean, zonal wind stress seasonal cycles were compared in the IndCen region (0-10°N, 60°E-80°E). Here the observations have a large monsoonal seasonal range, being westerly from April-October (peaking near $0.08\ \mathrm{Nm^{-2}}$ in June), and easterly from December-March, approaching $-0.03\ \mathrm{Nm^{-2}}$ in January. Of the 'no-adj' CGCMs, 6/8 have a westerly maximum that is less than 50% of that observed, and only BMRC and MPI match the observations at all well. IPSL-LR has very weak wind stress year-round. The 'adj' CGCMs perform better: all six have westerly onset as observed, and 5/6 have a westerly maximum larger than $0.05\ \mathrm{Nm^{-2}}$: GFDL-R30 is the exception, with a maximum less than half that observed.

4.3 VAT

The depth of averaging ranged from 300 to 400 m among the data submitted from 15 CGCMs, so it is difficult to compare VAT values. However it is useful to compare gradients and patterns: in the equatorial Pacific the annual mean zonal gradients of VAT (not

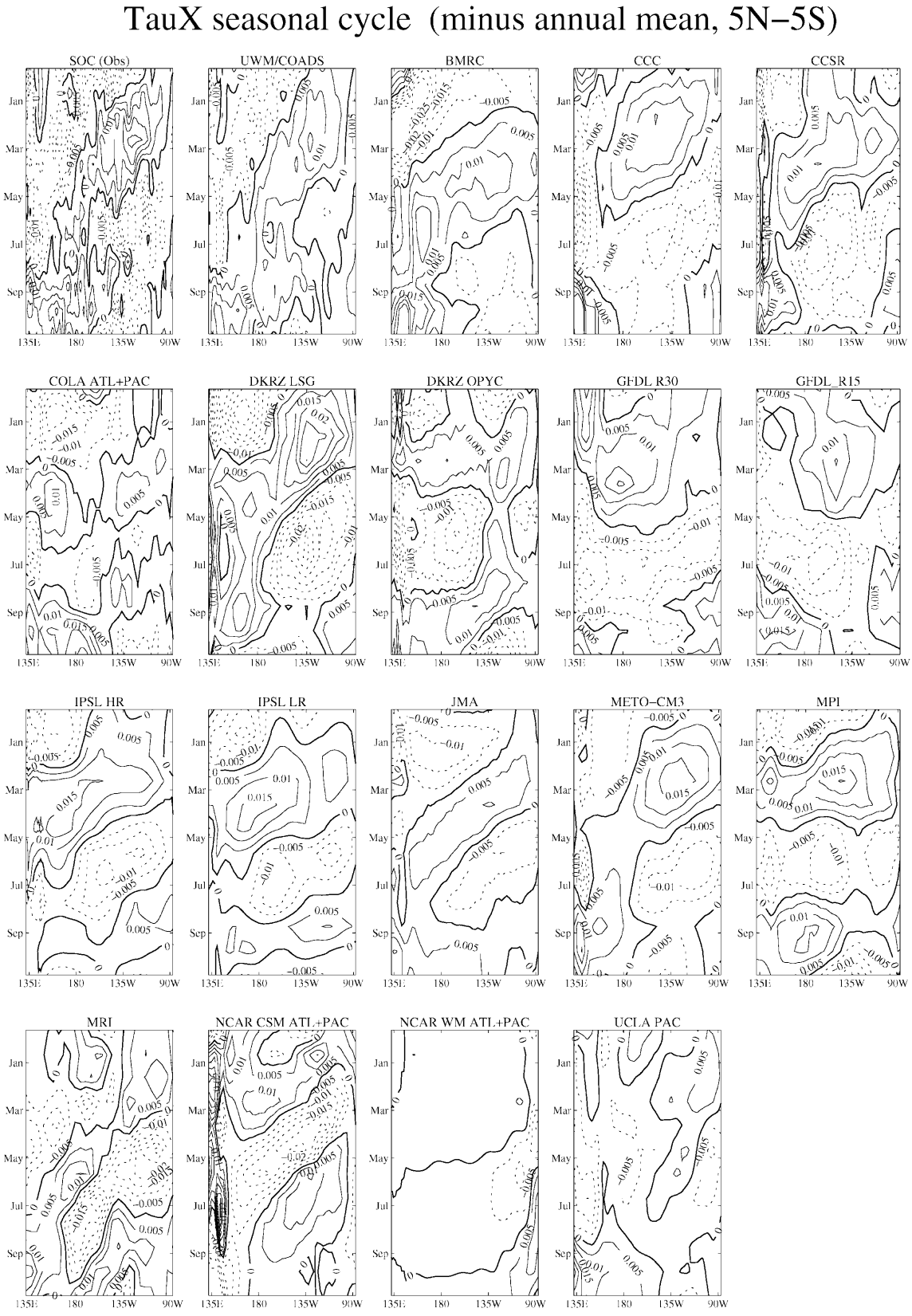

Fig. 3 Seasonal cycle of zonal wind stress (annual mean removed) in the equatorial strip (averaged 5°N-5°S), as observed and for the coupled models, for the Pacific regions. Units are N m^{-2}, with negative contours dashed. For *each panel* the *vertical axis* indicates month-of-year, while the *horizontal axis* indicates longitude

shown) all decrease from west to east at a rate similar to that observed. Time-longitude plots of the VAT seasonal cycle (with the annual mean removed) in the Pacific equatorial strip, averaged 5°N-5°S, are provided in Fig. 4. The observations suggest clear westward propagation of a dominant annual cycle in the central and west Pacific. The models generally do not reproduce this feature: only UCLA-PAC and METO-CM3 grossly resemble the observed propagation pattern, and both of these have deficiencies in places. The majority of the models have west-to-east propagation, in contrast to the observed behaviour, and several have seasonal ranges substantially weaker than that observed at most longitudes. Note that the observed seasonal range in VAT is quite small, being at most about 1°C in the central Pacific.

5 Levels of interannual variability

5.1 Pacific

Interannual equatorial Pacific SST behaviour is discussed in ENSIP2001: time-longitude maps for each model and tables of Niño3 and Niño4 standard deviations are provided therein, and the relationship to wind stress and VAT is explored. The results showed that only a few models could simulate the observed behaviour at all well. Here we provide some additional information by comparing wind stress and SST variability.

Figure 5 is a scatterplot of the standard deviation of interannual zonal wind stress anomalies in the PacCen region (5°N-5°S, 165°E-225°E) against that of SST′standard deviation in the Niño3 region. For many models the variability for both quantities is substantially lower than that observed: 13/20 have Niño3 SST standard deviations less than 70% of that observed, and 15/20 have PacCen wind stress standard deviations less than 70% of observed. (Bear in mind that observed values also fluctuate on decadal time-scales: 20-year segments from the GISST dataset give Niño3 values ranging from 0.6 to 1.0.) Only LAMONT has higher (almost double) values for both indices.

In these equatorial Pacific regions SST and wind stress anomalies are closely related, so the low model levels of interannual variability indicate low coupled variability. However, of the 12 CGCMs with Niño3 SST standard deviation larger than 0.4 °C, most have a ratio of wind stress to SST standard deviation substantially lower than that observed: for these models it seems that the low wind stress variability is not simply due to low coupled variability.

The nature and spatial distribution of the SST anomalies varies considerably between models (see Fig. 3 of ENSIP2001). Most of the 'no-adj' models at least have maximum SST′variability located somewhere in the central-east Pacific, but one (NCAR-CSM) has a maximum west of the dateline. Among the 'adj' models, HAWAII, GFDL-R30 and MRI have maxima located near the dateline. Although DKRZ-OPYC has Niño3 SST′variability close to that observed (Fig. 5), the spatial distribution has a peak that is larger (by over 50%) and narrower than observed. Maps of wind stress variability reveal that the low values in Fig. 5 reflect weak variability throughout the equatorial Pacific. Only the LAMONT model with a simple atmospheric component exceeds the observed variability, but its distribution is skewed to the east.

The low wind stress variability in the models could be simply due to underestimation of fluctuations on shorter time-scales, such as Madden-Julian oscillations. (Recall that monthly data are being analysed.) To investigate this possibility, the standard deviation calculations were repeated after applying a 7-month running mean to the observed and model data. Magnitudes were reduced by the filtering, but the outcome with regard to relative observed and model values was quite similar to the unfiltered result. The low model variances are not confined to the shorter time-scales.

5.2 Indian and Atlantic Oceans

In the other tropical oceans there is similarly a tendency for variability in the models to be lower than observed, but to a lesser extent. Variances averaged over representative equatorial regions are listed in Table 3. With regard to SST, in the Atlantic sector 7/18 CGCMs have interannual variance 50% lower than observed, and several have levels similar to observed. One exceptionally has variability much greater than observed. For the Indian Ocean sector most models have SST variance comparable to that observed: only 3/15 are below 50%, while 2/15 are more than double. NCAR-WM is unusual in having very high variance in the Indian and Atlantic regions, but relatively low variance over most of the equatorial Pacific.

With regard to zonal wind stress variance, Table 3 indicates that just 2/17 CGCMs have less than half the observed variance in the Atlantic sector, but 5/13 are below 50% in the Indian ocean sector. None has variance more than double that observed in either region.

6 Interannual connections with the equatorial Pacific

The observed ENSO cycle in the equatorial Pacific is associated with anomalies in other tropical and extratropical areas. Such connections have been extensively analysed in historical records of e.g. surface pressure, rainfall, temperature and winds, and investigated in numerical models. In this section we analyse the ability of the models to capture some observed tropical local and remote SST and wind stress features associated with ENSO variability. Observed behaviour has been documented by e.g. Rasmusson and Carpenter (1982), Tourre and White (1995), Harrison and Larkin (1998),

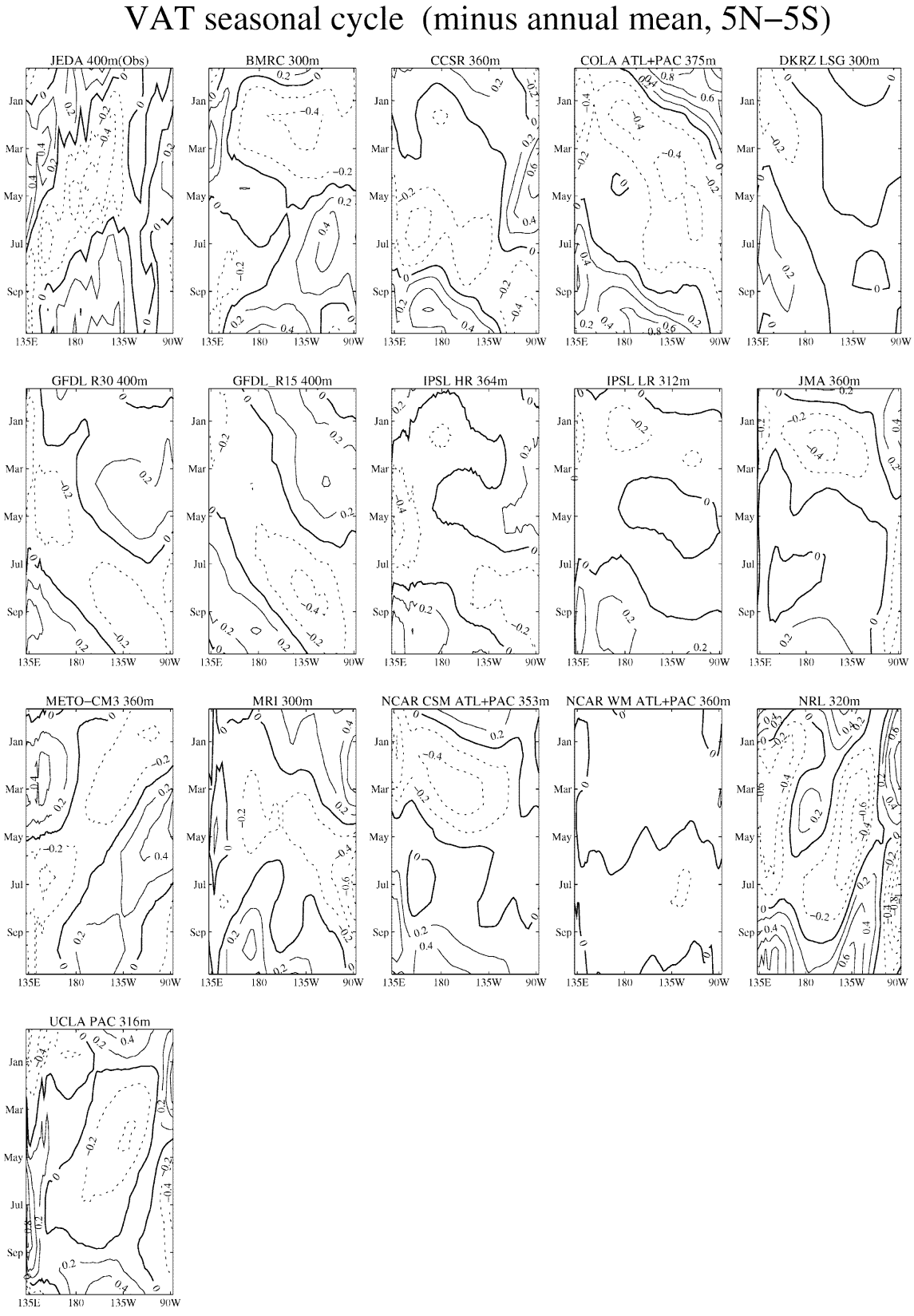

Fig. 4 Seasonal cycle of vertically averaged temperature (annual mean removed) in the equatorial strip (averaged 5°N-5°S), as observed and for the coupled models, for the Pacific ocean. Units are degrees C, with *negative* contours *dashed*. For each *panel* the *vertical axis* indicates month-of-year, while the *horizontal axis* indicates longitude

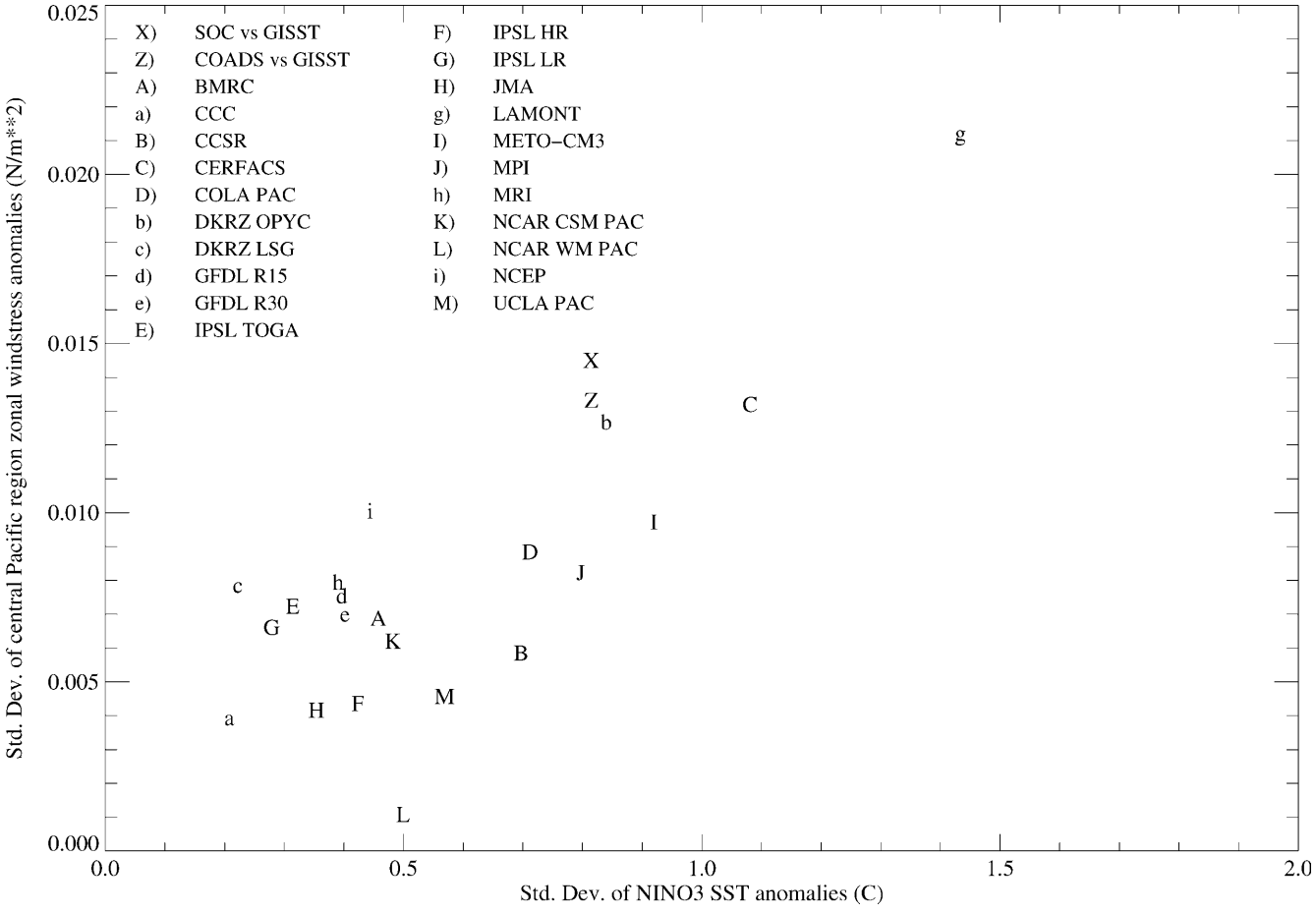

Fig. 5 Scatterplot of interannual standard deviations of SST (degrees C) in region Niño3 and zonal wind stress (N m^{-2}) in the central equatorial Pacific (5°N-5°S,165°E-225°E). *Lower case symbols* indicate models with flux adjustment, while *X* and *Z* indicate observed values

Nicholson (1997), Zhang and Levitus (1997), among many others. Lag correlations between Pacific SST and the other tropical oceans have also been widely investigated see e.g. Hameed et al. (1993), Enfield and Mayer (1997), Lanzante (1996), and Nicholson (1997).

The Niño3 SST′field is selected as a focal point for this analysis because it is a commonly used index for observed Pacific interannual fluctuations and connections. Although the spatial distribution of SST′variability differs widely between models, the temporal behaviour in Niño3 is generally characteristic of temporal behaviour over most of the equatorial Pacific in each model.

6.1 Correlations with Niño3 SST′

Correlations between SST′and Niño3 SST′(abbreviated as corr3 henceforth) were calculated for the models and for several multi-decadal segments of the GISST3 data. The main robust observed tropical features in spatial maps of corr3 in the Pacific region are: (a) corr3 $> +0.8$ over most of the region 5°N-5°S, east of the dateline; (b) corr3 < -0.3 in the west Pacific (west of 150°E near the equator), and in a large horseshoe shape which extends eastward from the equatorial west Pacific to around 40°N,140°W and 30°S,120°W; (c) corr3 $> +0.4$ along the Mexico/USA coast ($> +0.3$ up to Alaska). In the Indian Ocean: corr3 $> +0.3$ over most of the tropics, but weakly negative northwest of Australia; for the central Indian region, corr3 approaches $+0.5$ for lag $+6$ months (Niño3 leading). In the Atlantic Ocean: (a) corr3 is weak in the equatorial Atlantic (less than $+/-0.1$); (b) corr3 $> +0.2$ over most of the 10°N-30°N belt, with corr3 near $+0.4$ for lag $+6$ months; (c) corr3 $> +0.2$ over much of 20°S-30°S belt.

Correlations were likewise calculated for the models: principal results for select regions are provided in Table 4. For most models the positive corr3 values in the central-east equatorial Pacific erroneously extend across the equatorial western Pacific, and they fail to reproduce the observed negative correlations there. From the results for that region (PacW in Table 4), only 4/23 models have negative corr3. Of these four, only UCLA-PAC is from the 'no-adj' group.

With regard to the Pacific horseshoe pattern of negative correlations, only five (CCC, DKRZ-LSG, GFDL-

Table 3 Variances of interannual anomalies, averaged over the regions SSTAtl (2°N-2°S,320°E-350°E), SSTInd (2°N-2°S,60°E-90°E), TauAtl (5°N-5°S,320°E-350°E) and TauInd (5°N-5°S,60°E-90°E)

	SSTAtl	SSTInd	TauAtl	TauInd
GISST 61-90	0.23	0.14		
COADS			73	260
Model				
BMRC	0.22	0.13	64	220
CCC	0.03[a]	0.06[a]	20[a]	100[a]
CCSR	0.20	0.34[b]	53	120[a]
CERFACS	ND	ND	ND	ND
COLA	0.21	ND	50	ND
DKRZ-OPYC	0.04[a]	0.07[a]	70	420
DKRZ-LSG	0.09[a]	0.16	59	230
GFDL-R15	0.11[a]	0.18	91	220
GFDL-R30	0.17	0.22	44	100[a]
HAWAII	ND	ND	ND	ND
IPSL-TOGA	ND	ND	ND	ND
IPSL-HR	0.26	0.16	54	130
IPSL-LR	0.11[a]	0.12	78	150
JMA	0.11[a]	0.05[a]	23[a]	98[a]
LAMONT	ND	ND	ND	ND
METO-CM3	0.34	0.16	113	200
MPI	0.23	0.17	72	350
MRI	0.15	0.56[b]	38	90[a]
NCAR-CSM	0.20	ND	95	ND
NCAR-WM	1.66[b]	0.72[b]	104	ND
NCEP	ND	ND	ND	ND
NRL	0.11[a]	0.24	ND	ND
UCLA	0.18	ND	39	ND

Units are C^2 for SST variance and $(1000\ Nm^{-2})^2$ for wind stress variance. ND indicates No Data
[a]indicates value less than 50% of that observed
[b]indicates value more than twice that observed

R30, MRI, METO-CM3) out of the 15 models providing data for this region produced a clear negative horseshoe shape, with northern and southern arms connected across the equator, but not necessarily located as observed. (The success of CCC and DKRZ-LSG is notable in this regard, as these two models have the lowest Niño3 SST′variability.) The north and south Pacific area averages PacN and PacS in Table 4 provide a more quantitative measure of the off-equatorial behaviour. The observed correlations are substantially and robustly negative in these areas. For PacN (observed −0.3) only 7/15 models have correlations near or below −0.1 and only HAWAII reaches −0.2; while for PacS (observed −0.4) 9/15 have correlations near or below −0.1 and only CCC and MRI reach −0.3. While part of the failure to reproduce the horseshoe can be attributed to mis-location of equatorial variability, the results also suggest that many models do not properly represent the ocean-atmosphere processes that connect the equatorial and mid-latitude Pacific ocean regions.

In the Pacific the models also largely fail to capture the observed band of positive correlations that stretches north along the American coast. No model produced correlations greater than +0.3 in this area, and only 5 out of 15 (BMRC, CCC, DKRZ-OPYC, JMA, NCAR-WM) have a band of weakly positive correlations extending north from the equator (not shown).

Of the 14 models providing Indian ocean SST data, 7 (CCC, CCSR, GFDL-R30, JMA, MPI, METO-CM3) have Niño3 SST′correlations greater than +0.2 over most of the tropical Indian region, qualitatively as observed. To explore the Indian-Pacific relationship further, lag correlations between the IndCen and Niño3 regions were calculated. There is a very robust observed signal: 20-year segments throughout the GISST3 dataset consistently produced correlations over +0.4 in the range 0 to +9 months (Niño3 leading), and most samples also had weakly negative values at −12 months. The models largely fail to reproduce this feature: only JMA, MPI and METO-CM3 have peak values comparable to observations for positive lags, and the remainder have substantially weaker values (see Table 4). A few models have negative correlations at 0 lag in Table 4: this behaviour was generally associated with equatorially-confined tongues of negative correlation evident in spatial maps (not shown).

Observed correlations between Niño3 and the equatorial Atlantic are weak: there is a tendency for a small ($< +0.2$) positive correlation when Niño3 leads by several months, but the connection is not consistent with regard to amplitude or timing in different 20-year segments. This inconsistency reflects differing equatorial Atlantic responses (in timing and magnitude) to individual Pacific ENSO events, and may be partly due to independent Atlantic activity. Hence for the Atlantic Ocean, we focus on the north tropical region AtlN where there is a robust observed lag signal. Observed correlations between the AtlN and Niño3 regions reveal a consistent peak of about +0.4 around +6

Table 4 Correlations of interannual SST anomalies in other regions with SST anomalies in region Niño3, rounded to nearest 0.1

	PacW	PacN	PacS	IndCen −12	IndCen	IndCen +6	AtlN 0	AtlN+6
GISST 71-90	−0.2	−0.3	−0.4	−0.3	+0.5	+0.5	+0.2	+0.4
Model								
BMRC	+0.4	+0.1	+0.1	−0.1	+0.2	+0.2	0.0	+0.2
CCC	−0.1	−0.1	−0.3	−0.1	0.0	+0.1	+0.3	+0.3
CCSR	+0.3	−0.1	−0.2	+0.2	−0.2	−0.2	+0.2	+0.2
CERFACS	+0.1	ND	ND	ND	ND	ND	ND	ND
COLA	+0.1	ND	ND	ND	ND	ND	+0.1	+0.2
DKRZ-OPYC	+0.1	0.0	−0.2	−0.2	0.0	+0.3	+0.2	+0.6
DKRZ-LSG	+0.1	−0.1	0.0	−0.3	+0.1	+0.1	+0.2	+0.2
GFDL-R15	+0.1	−0.1	0.0	0.0	+0.1	+0.3	+0.3	+0.2
GFDL-R30	+0.1	0.0	−0.1	−0.2	−0.1	0.0	+0.4	+0.3
HAWAII	−0.1	−0.2	−0.2	ND	ND	ND	ND	ND
IPSL-TOGA	+0.3	ND	ND	ND	ND	ND	ND	ND
IPSL-HR	+0.5	+0.4	+0.3	+0.5	+0.3	+0.1	TR	TR
IPSL-LR	+0.3	ND	ND	−0.1	0.0	+0.2	ND	ND
JMA	+0.5	+0.1	+0.1	0.0	+0.4	+0.4	+0.2	+0.2
LAMONT	+0.3	ND	ND	ND	ND	ND	ND	ND
METO-CM3	+0.4	−0.1	−0.1	−0.3	+0.2	+0.6	+0.2	+0.3
MPI	+0.1	0.0	0.0	+0.1	+0.3	+0.5	+0.1	+0.3
MRI	0.0	−0.1	−0.3	+0.1	−0.2	−0.1	0.0	+0.1
NCAR-CSM	+0.3	ND	ND	ND	ND	ND	+0.3	+0.1
NCAR-WM	+0.3	0.0	−0.1	−0.3	−0.1	−0.1	+0.5	+0.4
NCEP	−0.1	ND	ND	ND	ND	ND	ND	ND
NRL	+0.5	+0.1	−0.2	ND	ND	ND	ND	ND
UCLA	−0.3	ND	ND	ND	ND	ND	ND	ND

In the region label, −12 indicates Niño3 lagging by 12 months, +6 indicates Niño3 leading by 6 months. ND indicates no data, TR indicates there was a trend in the data

months (Niño3 leading), with values around +0.2 at 0 lag and small negative correlations from −18 to −6 months lag. By contrast to the Indian Ocean connection, most models do broadly capture the weakly positive lag correlation pattern observed for AtlN: 12/14 have corr3 of +0.1 or more at 0 lag, and +0.2 or more at +6 months (see Table 4). The AtlN lag pattern is robust among several observed 20 year samples, but the model results are less reliable due to the small sample sizes.

6.2 Composite wind stress anomalies

The relatively noisy character of the wind stress fields made it difficult to find consistent signals by calculating correlations between SST indices and wind stress. A more effective approach was to calculate composites from observations and the coupled models, based on the Niño3 SST′timeseries. For the TOTAL composite, wind stress anomalies are averaged using all months with Niño3 SST′above +1 and (with reversed sign) below −1 standard deviation, while for WARM and COLD composites just the months above +1 and below −1 are used respectively. For the observations, the 20-year period 1970-89 was used.

The observed TOTAL wind stress composite has several typical and well-known features: westerly anomalies in the central equatorial Pacific with flanking convergent equatorward motion; northerly anomalies north of the equator in the east Pacific; westerly anomalies in the north and south mid-latitude Pacific; easterly anomalies in the east equatorial Indian Ocean; easterly anomalies in the tropical north Atlantic. Harrison and Larkin (1998) have provided a much more detailed composite analysis of the ENSO cycle. Most of the wind stress features described here broadly match their 'peak phase' features. (See e.g. plate 6 of Harrison and Larkin 1998.)

We have summarised the model behaviour by selecting regions with a distinct observed composite signal and assessing the ability of the models to reproduce the observed features. Area averages for several regions (defined in Table 2) were calculated. Table 5 provides information about the observed composite for each area, and indicates for each model and area whether or not the wind stress composite has the same sign as that observed. (From individual maps, not shown, the sign is a reasonable indicator of the presence of a feature as wind direction was generally consistent within the selected areas.)

The observed composite signal does not necessarily occur during all WARM and COLD episodes. The robustness was checked by calculating area averages for 8 individual events observed in the 20-year period 1970-89, and the robustness scores are included in Table 5. Harrison and Larkin (1998) discuss issues of robustness in more detail. Due to the small sample sizes, the results here should be regarded as qualitative. The expectation is that in areas with robust observed signals the models should reproduce the observed features.

In the equatorial Pacific (EqPac1, EqPac2, EqPac3, Epac) nearly all the models have TOTAL composites with the correct sign. Despite the widely varying interannual behaviour of the individual models, the wind stress response to warming/cooling in Niño3 SST is qualitatively like that observed. Most of the models also capture the mid-latitude Pacific westerly features (NPac, SPac), and the equatorial Indian Ocean easterlies (EqInd). The models evidently reproduce the main remote wind stress signals qualitatively well. In the south Indian Ocean (SInd), nearly all the models have a consistent westerly TOTAL wind stress composite. The observed TOTAL composite is quite weak: for the years sampled, the observed signal comes predominantly from a consistent easterly signal during COOL events.

The WARM composite is provided for the equatorial Atlantic region (EqAtl). While there is a clear easterly WARM composite signal, the observed COOL composite is very weak. Most models likewise had very weak COOL composite values. The models apparently qualitatively reproduce the observed asymmetry between WARM and COOL effects in this area.

7 Summary and conclusions

Through the comparison of observations and 23 coupled ocean-atmosphere models with widely varying components and configurations, behaviour of SST, zonal wind stress and VAT in tropical ocean regions has been analysed. The main results, which update and extend previous assessments that focused on Pacific SST, are summarised and discussed later.

7.1 Annual mean and annual cycle

With regard to annual mean equatorial SST (Fig. 1), the clear deficiencies evident in most of the CGCMs with no 'flux adjustment' are (a) too cool, by 2 to 3 °C, in much of the equatorial Pacific and (b) wrong east-west gradient in the equatorial Atlantic. Most also have a too-prominent equatorial cold trough in the east Pacific and the central Atlantic. In the eastern equatorial Pacific and Atlantic substantial warm SST biases are evident in most of the 'no-adj' CGCMs. However, all models do have a strong west-east SST gradient in the central Pacific similar to that observed. Several common biases also appear in the annual mean equatorial zonal wind stress (Fig. 2). Most of the models, with and without adjustment, have easterlies too weak in the equatorial Atlantic and westerlies too weak in the Indian sector. Among the 'no-adj' CGCMs, most have easterly wind stress too weak in the central equatorial Pacific, but easterly wind stress too strong in the west equatorial Pacific, leading to a west-central Pacific gradient much lower than observed.

Table 5 Interannual wind stress anomaly composite results

	EqPac1	EqPac2	EqPac3	EPac	NPac	SPac	EqInd	SInd	EqAtl (Warm)
COADS > strength	Zonal +.007	Merid. −.010	Merid. +.003	Merid. −.004	Zonal +.012	Zonal +.013	Zonal −.007	Zonal +.001	Zonal −.004
robustness	8/8	8/8	7/8	6/8	7/8	8/8	7/8	6/8	
Model									
BMRC	*	*	*	*	*	*	*	*	*
CCC	*	*	X	*	X	*	*	*	*
CCSR	X	*	*	*	*	*	*	*	*
CERFACS	*	*	*	*	ND	ND	ND	ND	ND
COLA	*	*	*	*	ND	ND	ND	ND	ND
DKRZ-OPYC	*	*	*	*	*	*	*	*	*
DKRZ-LSG	*	*	*	*	*	*	X	*	*
GFDL-R15	*	*	X	X	*	*	*	*	*
GFDL-R30	*	*	*	X	*	X	*	*	*
HAWAII	ND	ND	ND	ND	ND	ND	ND	ND	ND
IPSL-TOGA	*	*	*	*	ND	ND	ND	ND	ND
IPSL-HR	*	*	*	*	*	*	*	*	*
IPSL-LR	*	*	*	*	ND	ND	X	ND	X
JMA	*	*	*	*	*	X	*	X	*
LAMONT	*	*	X	*	ND	ND	ND	ND	ND
METO-PRE	*	*	*	*	*	*	*	*	*
METO-CM3	*	*	*	*	*	*	*	*	*
MPI	*	*	*	*	*	*	*	*	*
MRI	*	*	*	*	*	*	*	*	*
NCAR-CSM	*	*	*	*	ND	ND	*	ND	ND
NCAR-WM	*	X	*	*	ND	ND	ND	ND	ND
NCEP	*	*	*	*	ND	ND	ND	ND	ND
NRL	ND	ND	ND	ND	ND	ND	ND	ND	ND
UCLA-PAC	*	*	*	*	ND	ND	ND	ND	ND

The selected wind stress component is indicated with the observed value in Nm^{-2}. *indicates model composite has same sign as that observed, X indicates model has opposite sign, ND means no data available

With regard to the Pacific, the mean equatorial SST errors are quite similar to those found in previous CGCM comparisons, see Fig. 1 of Mechoso et al. (1995) – with a marked tendency for the cold tongue to be too narrow and too strong. Mechoso et al. (1995) comment that mean equatorial wind stresses were underestimated: the STOIC results provide detailed evidence that these errors still prevail, with too-weak central Pacific easterly wind stress accompanying too-cold SST in most of the 'no-adj' group. As many of the OGCMs use basically the same mixing and advective schemes as in the Mechoso et al. (1995) CGCM sample, it seems likely that errors in representing upper ocean equatorial mixing and circulation (compounded by ocean-atmosphere interaction and feedbacks) continue to lead to these equatorial biases. The warm biases in the eastern equatorial Pacific are another recurring feature noted in previous assessments. These, and similar warm biases in the east equatorial Atlantic, are likely to be associated with deficiencies in the representation of low level stratus cloud, as found in Mechoso et al. (1995).

The equatorial annual cycle of SST in the Pacific is discussed in detail in ENSIP2001: a common deficiency is for the annual cycle in the eastern Pacific to be too weak. In the equatorial Atlantic and Indian oceans most models performed quite well with regard to phase and location of maxima and minima features. However, as in the Pacific, annual cycles tend to be weaker than observed, and semi-annual components are in some cases stronger than observed.

Errors were more evident in the zonal wind stress annual cycle, for which many of both the 'adj' and 'no-adj' models have similar and substantial deficiencies in the various equatorial sectors. In the central equatorial Atlantic very few models could simulate the observed cycle, and in the central Indian Ocean, the majority of the models could not match the strength of the observed June-July westerly maximum. In the equatorial Pacific (Fig. 3) several 'no-adj' and 'adj' models have semiannual signals that are much stronger than observed.

With regard to VAT, in the equatorial Pacific (Fig. 4) very few of the CGCMs that provided VAT data were able to reproduce the observed east-to-west propagation pattern in the annual cycle, and the majority had west-to-east propagation. The range of the observed cycle is small (less than 1 °C when the average is over the top 400 m of the ocean), so the significance of this deficiency is not clear. Nevertheless, the relationship between wind stress and VAT in most models evidently differs from that observed: although the VAT propagation directions commonly are different from that observed, most models have an annual east-to-west zonal wind stress propagation pattern like that observed.

7.2 Interannual variability

Equatorial Pacific SST interannual variability is described in detail in ENSIP2001: few models produced good simulations with regard to level, form and location, and few could be said to have realistic ENSO-like behaviour. Levels of CGCM SST variability in the Indian Ocean were comparable to observations, but tended to be too low in the equatorial Atlantic. Levels of zonal wind stress interannual variability in most of the CGCMs were considerably lower than observed in the central equatorial Pacific. Often the shortfall in Pacific variability was more pronounced for zonal wind stress than for SST, which suggests that ways of boosting wind stress activity in the atmospheric components need to be sought.

Correlations between SST and Niño3 SST anomalies were used to investigate teleconnection features. In the Pacific the observational map has a distinctive and robust horseshoe pattern of negative correlations which only a few models could reproduce. Failure to capture the west equatorial Pacific part of the horseshoe is partly a consequence of placing largest SST variability too far to the west. In most models connections with off-equatorial Pacific regions were weaker than observed. While a few of the 'no-adj' models captured the robust observed lag relationship with the Indian Ocean (Pacific leading by several months), none of the 'adj' models reproduced this feature. In this aspect the models performed better in the Atlantic sector, with most models having a positive correlation with part of the north tropical Atlantic, as observed, and several also had a semblance of the observed lead-lag relation. Inability to represent these teleconnections well may be due to several factors, such as the relatively low levels of Pacific variability in many models and the improper location of maximum atmospheric heating in latitude, longitude and height during interannual events.

Although it was difficult to find robust wind signals via correlations, the use of wind stress composites based on episodes of relatively high and low Niño3 SST anomalies proved to be effective. There are several distinctive observed composite features in the tropics, and most of the models performed quite well in terms of reproducing these features, at least in terms of sign. As with SST variability, magnitudes of the wind stress composites were generally low.

With regard to interannual variability overall, the 'no-adj' group tended to perform better than the 'adj' group. Part of the explanation for this difference is likely to be that the 'no-adj' models generally had higher resolution than the 'adj' models, particularly in the near-equatorial ocean regions, which in turn reflects a greater emphasis placed on tropical behaviour in the design and purpose of the 'no-adj' group.

7.3 Conclusions

From the evidence in the STOIC and ENSIP results, the equatorial Pacific is still a major problem area for coupled models. In CGCMs with no form of flux adjustment

a drift to too-cold equatorial SST remains the main common climatological error, and most models do not simulate Pacific interannual activity well. Mean SST has emerged as a concern in the equatorial Atlantic sector, with only one model producing the right zonal gradient in the 'no-adj' group. Surface wind stress is a major problem with regard to the seasonal climatology in all ocean sectors and levels of variability in the Pacific, for both 'adj' and 'no-adj' models. As models in the 'adj' group generally have an SST climatology kept close to that observed, these errors cannot simply be attributed to coupled drift: improvements in the atmospheric components are clearly needed. The limited analysis of VAT revealed common errors in the Pacific seasonal cycle. Overall, no single model is consistent with observed behaviour in the tropical ocean regions. Understanding and overcoming these shortcomings must be a high priority for the coupled modelling community.

The question arises as to whether the 20-year samples are adequate. Based on the analysis of samples of GISST3 SST, the comparison of SOC and COADS wind stresses, and a variety of CGCM data, the 20-year samples used here are adequate for assessing annual mean and seasonal cycle behaviour; particularly as the model biases are large and gross errors are readily apparent. The samples also seem adequate for assessing the dominant features in patterns of variability, and for determining gross errors in levels of variability. However, the reliability of the quantitative results is questionable, as both models and observations vary on decadal and longer timescales. For future such comparisons, 100-year or longer model samples would be preferable to increase the reliability of assessments of interannual variability. The problem of determining the 'real world' range of interannual behaviour from limited datasets still remains.

Acknowledgements K.R. Sperber was supported under the auspices of the US Department of Energy Environmental Sciences Division at the Lawrence Livermore National Laboratory under Contract W-7405-ENG-48. We thank Nick Rayner (Met Office) and Simon Josey (Southampton Oceanography Centre) for making pre-release versions of their observational datasets available.

Appendix A

Further model details

While the CGCMs use a wide variety of atmospheric components, the majority of the oceanic components are variations of the Bryan/Cox model (Bryan 1969; Cox 1984) from GFDL (Geophysical Fluid Dynamics Laboratory, USA). Four CGCMs (CERFACS and IPSL-TOGA/HR/LR) use variations of the OPA OGCM (Delecluse et al. 1993) from IPSL/LODYC (IPSL, Institut Pierre Simon Laplace, LODYC, Laboratoire d'Oceanographie Dynamique et de Climatologie, France). MPI, DKRZ-OPYC, DKRZ-LSG and NCAR-CSM use other OGCMs as detailed below. LAMONT and HAWAII use highly simplified reduced-physics components.

BMRC: Bureau of Meteorology Research Centre (Australia); CGCM described in Power et al. (1998).

CCC: Canadian Centre for Climate Modelling and Analysis; CGCM described in Flato et al. (1998) ; monthly varying flux adjustments for heat and fresh water used.

CCSR: Center for Climate System Research (Japan); CGCM described in Watanabe et al. (1999); SST is relaxed to observed climatology poleward of latitude 55.

CERFACS: European Centre for Research and Advanced Training in Scientific Computation (France); CGCM described in Terray (1998).

COLA: Centre for Ocean-Land-Atmosphere Studies (USA); CGCM described in Dewitt and Schneider (1999).

DKRZ: Deutsches Klimarechenzentrum. The DKRZ-OPYC CGCM is described in Bacher et al. (1998), uses an isopycnic OGCM (Oberhuber 1993); annual mean flux adjustment for heat and fresh water.

The DKRZ-LSG CGCM described in Voss et al. (1998), a large-scale geostrophic OGCM (Maier-Reimer et al. 1993); monthly varying flux adjustment for momentum, heat and fresh water.

GFDL: Geophysical Fluid Dynamics Laboratory (USA). The GFDL-R15 CGCM is described in Manabe et al. (1991), while GFDL-R30 is described in Knutson et al. (1998). Both use monthly varying flux adjustment for momentum, heat and fresh water.

HAWAII: University of Hawaii (USA); simplified physics tropical model described in Wang and Fang (2000).

IPSL: IPSL-TOGA is the CGCM described in Vintzileos et al. (1999).

IPSL-LR is the CGCM described in Braconnot et al. (1997); IPSL-HR uses the same AGCM as IPSL-LR, but with 15 rather than 11 levels, and the same OGCM as IPSL-LR but with double the horizontal resolution.

JMA: Japan Meteorological Agency; CGCM described in Yoshikawa et al. (1995): the Arctic ocean and sea-ice are not included.

LAMONT: Lamont Doherty Earth Observatory (USA); simplified physics tropical Pacific model described in Zebiak and Cane (1987).

METO: the Met Office (UK); METO-CM3 is the Hadley Centre CGCM, known as HADCM3, described in Gordon et al. (2000) and Collins et al. (2001).

MPI: Max Planck Institute for Meteorology (Germany); CGCM described in Frey et al. (1997) uses HOPE (Hamburg Ocean model in Primitive Equations, Wolff et al. 1996), with prescribed sea ice.

MRI: Meteorological Research Institute (Japan); CGCM described in Yukimoto et al. (1996); monthly varying flux adjustment for heat and fresh water.

NCAR: National Center for Atmospheric Research (USA). NCAR-WM is the CGCM described in Washington and Meehl (1996). NCAR-CSM is the CGCM described in Boville and Gent (1998), which uses the NCAR OGCM.

NCEP: National Centers for Environmental Prediction (USA); CGCM described in Ji et al. (1998), with one-way anomaly coupling from AGCM to OGCM.

NRL: Naval Research Laboratory (USA); CGCM described in Li and Hogan (1998).

UCLA: University of California, Los Angeles (USA); CGCM described in Mechoso et al. (2000). UCLA-PAC has a global AGCM coupled to a

tropical Pacific OGCM, while UCLA-ATL has an earlier version of the global AGCM coupled to a tropical Atlantic OGCM.

References

AchutaRao K, Sperber KR and the CMIP modelling groups (2001) El Niño Southern Oscillation in coupled GCMs. Clim Dyn

Bacher A, Oberhuber JM, Roeckner E (1998) ENSO dynamics and seasonal cycle in the tropical Pacific as simulated by the ECHAM4/OPYC3 coupled general circulation model. Clim Dyn 14: 431–450

Boville BA, Gent PR (1998) The NCAR climate system model, version one. J Clim 11: 1115–1130

Braconnot P, Marti O, Joussaume S (1997) Adjustment and feedbacks in a global coupled ocean-atmosphere model. Clim Dyn 13: 507–519

Bryan K (1969) A numerical method for the study of the circulation of the world ocean. J Comp Phys 4: 347–376

Collins M, Tett SFB, Cooper C (2001) The internal climate variability of a HadCM3: a version of the Hadley Centre coupled model without flux adjustments. Clim Dyn 17: 61–81

Cox MD (1984) A primitive equation three-dimensional model of the ocean. GFDL Ocean Group Tech. Rep 1

Da Silva AM, Young CC, Levitus S (1995) Atlas of surface marine data 1994, volume 1: algorithms and procedures. NOAA Atlas NESDIS 6, US Department of Commerce

Davey MK, Huddleston M, Sperber KR (2000) The CLIVAR-WGSIP STOIC project. CLIVAR Exchanges 17: 21–23

Delecluse P, Madec G, Imbard M, Levy C (1993) OPA version 7 ocean general circulation model reference manual. LODYC internal report 93/05

Delecluse P, Davey MK, Kitamura Y, Philander SGH, Suarez M, Bengtsson L (1997) Coupled general circulation modelling of the tropical Pacific. J Geophys Res 103 (C7): 14357–14373

DeWitt DG, Schneider EK (1999) The processes determining the annual cycle of equatorial sea surface temperature: a coupled general circulation model perspective. Mon Weather Rev 127: 381–395

Enfield DB, Mayer DA (1997) Tropical Atlantic sea surface temperature variability and its relation to El Niño Southern Oscillation. J Geophys Res 102 (C1): 929–945

Flato, GM, Boer GJ, Lee MG, McFarlane NA, Ramden D, Reader MC, Weaver AJ (2000) The Canadian Centre for Climate Modelling and Analysis global coupled model and its climate. Clim Dyn 16: 451–467

Frey H, Latif M, Stockdale T (1997) The coupled GCM ECHO2. Part 1: the tropical Pacific. Mon Weather Rev 125: 703–720

Gordon C, Cooper C, Senior CA, Banks H, Gregory JM, Johns TC, Mitchell JFB, Wood RA (2000) The simulation of SST, sea ice extents and ocean heat transports in a version of the Hadley Centre coupled model without flux adjustments. Clim Dyn 16: 147–168

Hameed S, Sperber KR, Meinster A (1993) Teleconnections of the Southern Oscillation in the tropical Atlantic sector in the OSU coupled upper ocean-atmosphere GCM. J Clim 6: 487–498

Harrison DE, Larkin NK (1998) El Niño Southern Oscillation sea surface temperature and wind anomalies 1946–1993. Rev Geophys 36: 353–399

Ji M, Behringer DW, Leetmaa A (1998) An improved coupled model for ENSO prediction and implications for ocean initialization. Part II: the coupled model. Mon Weather Rev 126: 1022–1034

Josey SA, Kent EC, Taylor PK (1999) The SOC ocean-atmosphere heat, momentum and fresh water flux atlas. Southampton Ocean Centre Rep 6.

Knutson TR, Manabe S (1998) Model assessment of decadal variability and trends in the tropical Pacific Ocean. J Clim 11: 2273–2296

Lanzante JR (1996) Lag relationships involving tropical sea surface temperatures. J Clim 9: 2568–2578

Latif M, Sperber K et al (2001) ENSIP – The El Niño simulation intercomparison project. Clim Dyn

Li T, Hogan TF (1998) The role of the annual-mean climate on seasonal and interannual variability of the tropical Pacific in a coupled GCM. J Clim 12: 780–792

Maier-Reimer E, Mikolajewicz U, Hasselmann K (1993) Mean circulation of the Hamburg LSG model and its sensitivity to the thermohaline surface forcing. J Phys Oceanog 23: 731–757

Manabe S, Stouffer RJ, Spelman MJ, Bryan K (1991) Transient responses of a coupled ocean-atmosphere model to gradual changes of atmospheric CO2. Part I: annual mean response. J Clim 4: 785–818

Mechoso C, Robertson AW et al (1995) The seasonal cycle over the tropical Pacific in general circulation models. Mon Weather Rev 123: 2825–2838

Mechoso CR, Yu J-Y, Arakawa A (2000) A coupled GCM pilgrimage: from climate catastrophe to ENSO simulations. In: Randall DA (ed). General circulation model development: past, present, and future. Academic, New York, pp 539–575

Meehl GA, Boer GJ, Covey C, Latif M, Stouffer RJ (2000) The Coupled Model Intercomparison Project (CMIP). Bull Am Meteorol Soc 81: 313–318

Neelin D, Latif M et al (1992) Tropical air-sea interaction in general circulation models. Clim Dyn 7: 73–104

Nicholson SE (1997) An analysis of the ENSO signal in the tropical Atlantic and western Indian oceans. Int J Clim 17: 345–375

Oberhuber JM (1993) Simulation of the Atlantic circulation with a coupled sea-ice mixed layer isopycnal general circulation model. Part 1: model description. J Phys Oceanog 13: 808–829

Power SB, Tseitkin F, Colman RA, Sulaiman A (1998) A coupled GCM for seasonal prediction and climate change research. BMRC Res Rep 66, 52 pp

Rasmusson EM, Carpenter TH (1982) Variations in tropical sea surface temperature and surface wind fields associated with Southern Oscillation/El Niño. Mon Weather Rev 110: 354–384

Rayner MA, Horton EB, Parker DE, Folland CK (1998) Versions 2.3b and 3.0 of the global sea-ice and sea surface temperature data set. Hadley Centre Internal Note 85

Terray L (1998) Sensitivity of climate drift to atmospheric physical parameterizations in a coupled ocean-atmosphere model. J Clim 11: 1633–1658

Tourre YM, White WB (1997) Evolution of the ENSO signal over the Indo-Pacific domain. J Phys Oceanog 27: 683–696

Vintzileos A, Delecluse P, Sadourny R (1999) On the mechanisms in a tropical ocean-global atmosphere coupled general circulation model. Part I: mean state and the seasonal cycle. Part II: interannual variability and its relation to the seasonal cycle. Clim Dyn 15: 43–80

Voss R, Sausen R, Cubasch U (1998) Periodically synchronously coupled integrations with the atmosphere-ocean general circulation model ECHAM3/LSG. Clim Dyn 14: 249–266

Wang B, Fang Z (2000) Roles of short-wave radiation forcing on ENSO: a study with an intermediate coupled ocean-atmosphere model. Clim Dyn 16: 677–691

Washington WM, Meehl GA (1996) High latitude climate change in a global coupled ocean-atmosphere-sea ice model with increased atmospheric CO2. J Geophys Res 101: 12795–12801

Watanabe M, Kimoto M, Kachi M, Nitta T (1999) A comparison of decadal climate oscillations in the North Atlantic detected in observations and a coupled GCM. J Clim 12:2920–2940

Wolff J-O, Maier-Reimer E, Legutke S (1996) The Hamburg Ocean Primitive Equation model HOPE. DKRZ Tech Rep 13

Yoshikawa I, Ishii M, Kimoto M (1995) Characteristics of JMA Coupled Ocean-Atmosphere model. Proc int workshop on

numerical prediction of oceanic variations. Tokyo, 7-11 March 1995, pp 189–194

Yukimoto S, Endoh M, Kitamura Y, Kitoh A, Motoi T, Noda A, Tokioka T (1996) Interannual and interdecadal variabilities in the Pacific in an MRI coupled GCM. Clim Dyn 12: 667–683

Zebiak SE, Cane MA (1987) A model El Niño-Southern Oscillation, Mon Weather Rev 115: 2262–2278

Zhang R-H, Levitus S (1997) Interannual variability of the coupled tropical Pacific ocean-atmosphere system associated with the El Niño-Southern Oscillation. J Clim 10: 1312–1330